

*Research article***Experiment of a new style oscillating water column device of wave energy converter****Frederick N.-F. Chou¹, Chia-Ying Chang^{1*}, Yang-Yih Chen¹, Yi-Chern Hsieh², and Chia-Tzu Chang¹**¹ Hydraulic and Ocean Engineering Department, National Cheng Kung University, Taiwan² Power Mechanical Engineering Department, National Formosa University, Taiwan* **Correspondence:** E-mail: n88991114@mail.ncku.edu.tw.

Abstract: In 1799, the first wave–power patent was filed. Since then, a significant amount of research has been done on the performance of an oscillating water column (OWC) using linear theory. In general, the use of linear theory has been found to be both judicious and accurate. We used experiment to know what happen in the OWC. A suitable analytical model for devices in shallow water is required to predict the effect of water depth on performance and to provide guidance in device optimization. Because of the lack of clarity in defining why linear theory becomes less accurate in shallow water, digital video recordings were used to analyze the flow around the OWC wave–energy converter. This provided detailed images that could be analyzed both temporally and spatially. The OWC’s operation qualitatively differs from that predicted by linear theory, identifying critical flow properties. This paper describes one depth flow and a discussion of its influence on the wave period.

Keywords: oscillating water column; renewable energy; wave energy; water wave; experiment

1. Introduction

Globally, there has been an increase in the search for “clean, socially acceptable methods of generating power” [1,2]. This is because of two interrelated factors: (1) the global requirement for electricity, which is expected to increase in the next 15 years, and (2) the promise by different countries to reduce their CO₂ emissions in the same time frame.[8] Some of the efforts undertaken by countries to increase the share of renewable energy in their energy consumption include the

setting of feed-in tariffs (FITs). While FITs are targeted at wind and solar energies, the generation of electricity from waves, tidal currents and tides has received renewed interest. [3]

There are different patterns of ocean energy: tidal and currents, waves, salinity, and thermal gradients [4,5]. Tidal energy from waves can be converted into electrical energy [6]. The generation of tidal energy depends on the tide altitude and tide velocity; higher tide altitudes and velocities will lead to higher electricity generation [7]. The kinetic and potential energy associated with ocean waves can be used at onshore or offshore sites using different wave–energy converter technologies [5,6].

The outflow rate of water contained in the chamber was then measured by an accurate and correctly calibrated velocity gauge. The experimental results were then applied, indicating a chamber design and geometry, which provides optimal energy output.

2. Materials and Method

The experimental setup consisted of an open channel of dimension $18 \times 0.5 \times 0.4 \text{ m}^3$ (Figure 1), equipped with a controllable wave generator placed at one end of the channel (Figure 2). An artificial seashore protected from returning waves was situated at the other end. An oscillating water column (OWC) was made from acrylic within an iron frame.

Suitably sealed material was used to prevent air and water leakage through the iron frame. As indicated, a tube was mounted at the side of the chamber to guide the air exiting the chamber toward the intake of the turbine.

All experimental readings were taken at the steady state factors. Water velocity readings were registered by a velocity gauge with a digital manometer (both instruments were accurately calibrated in the fluid mechanics laboratory).

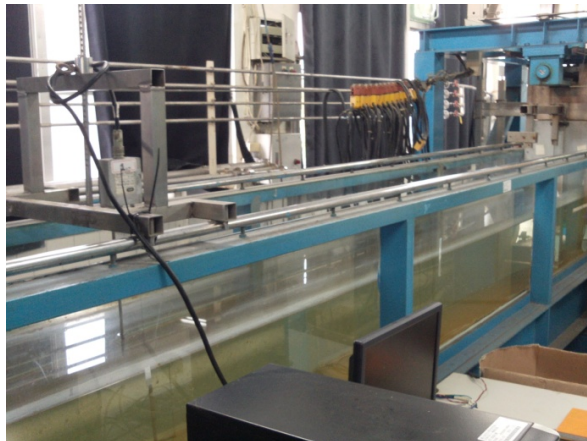


Figure 1. Open channel in the lab.

2.1. Theory

The wave generator is based on Airy's linear wave theory [Airy-1845].

The free-surface elevation can be defined as follows:

$$\eta = A \cos(kx - \omega t + \phi), \quad (1)$$

where k is the wave number, ω is the angular frequency, t is time, and ϕ is the phase shift angle.

The power of the outputted air is calculated from the following relationship:

$$P_w = \left(P + \frac{1}{2} \rho V^2 \right) VA, \quad (2)$$

where P_w is the water pressure at the inside of the channel, ρ is the water density, V is the internal flowing water velocity, and A is the area of the internal water model.



Figure 2. Wave maker in the lab.

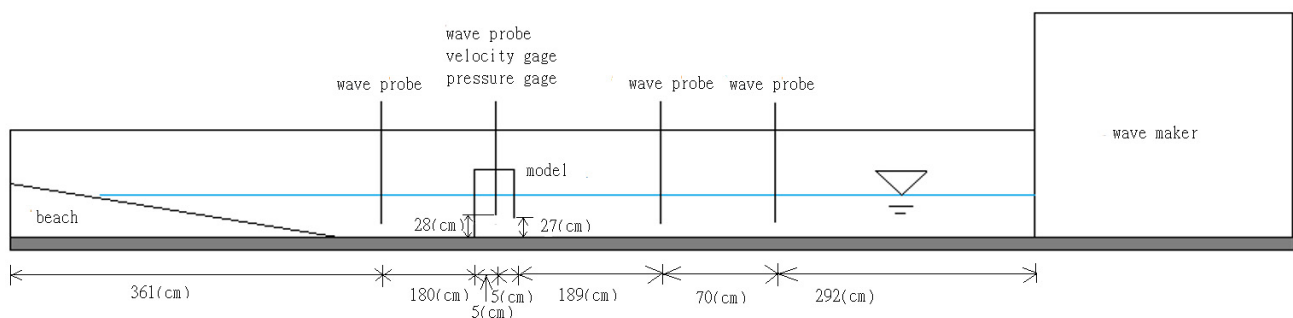
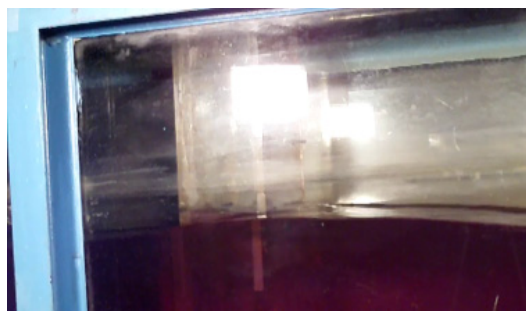


Figure 3. Schematic of the experimental setup illustrating: the position of the oscillating water column relative to the wave maker; the wave-probe positions; and the dimensions of the wave tank and model

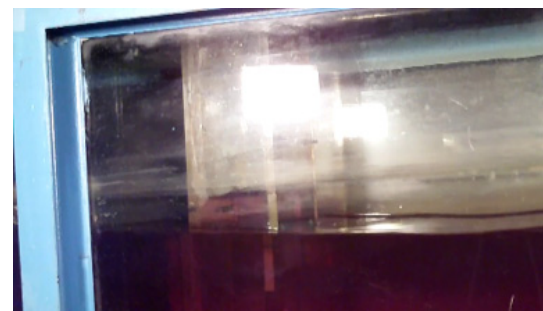
3. Results and Discussion

The water surface elevation varies at different location and are different among the front wall, center and rear wall of OWC in a wave period. The wave height in the chamber is greater than the incident wave amplitude as shown in Figures 4(a) and 4(h). The maximum height of the wave amplitude in the chamber is shown in Figures 4(b) and 6(e). The lowest run-down wave amplitude in the chamber is shown in Figures 4(c) and 4(g). The water level in the chamber wall begins to rise,

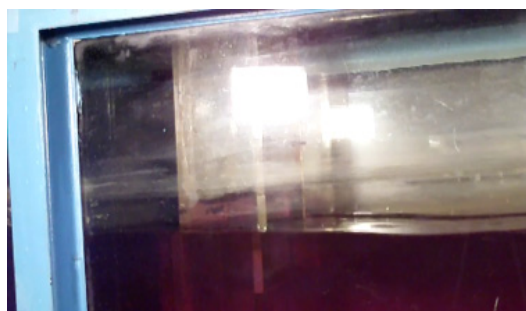
as shown in Figure 4(d). One can estimate wave energy from wave height, which can be computed from wave peak, figure 4(f).



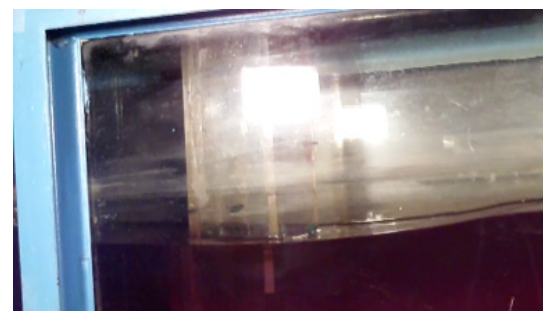
(a) $t_1 = 0$



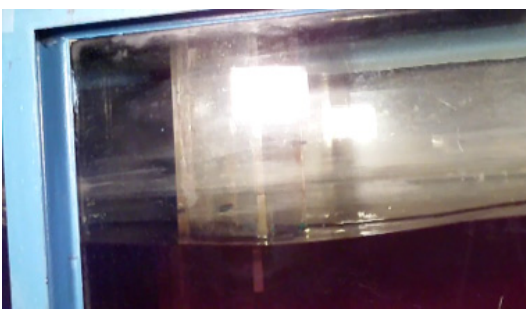
(e) $t_5 = 5T/4$



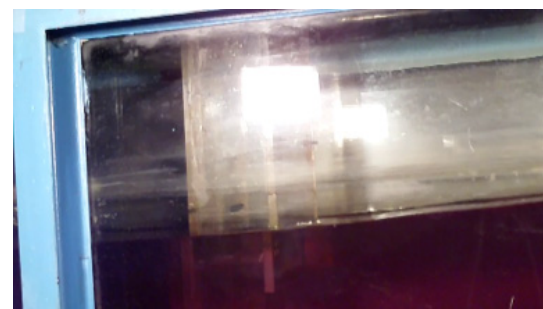
(b) $t_2 = T/4$



(f) $t_6 = 3T/2$



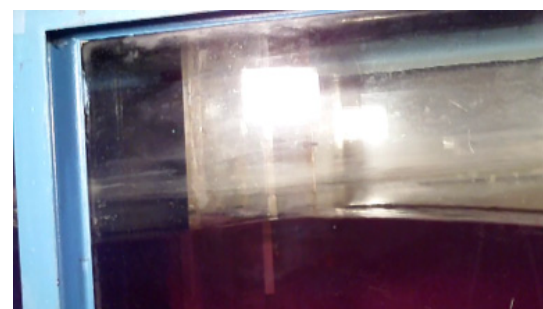
(c) $t_3 = T/2$



(g) $t_7 = 7T/4$

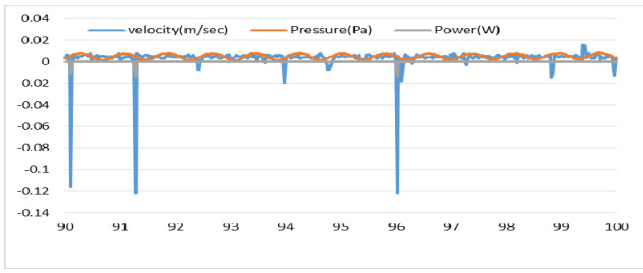


(d) $t_4 = T$

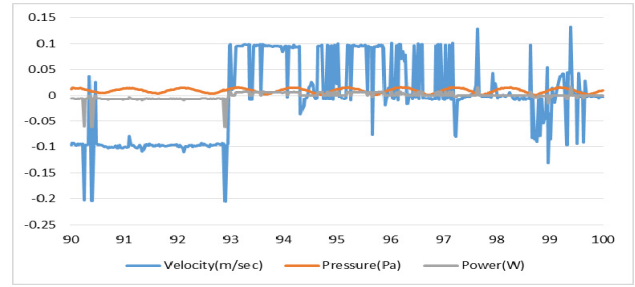


(h) $t_8 = 2T$

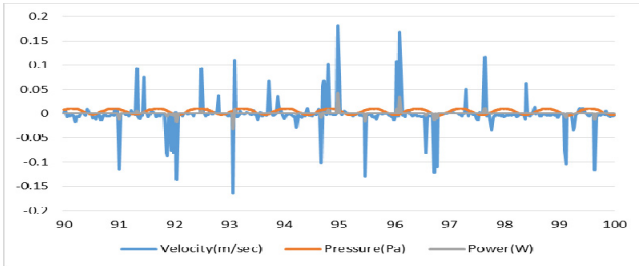
Figure 4. Digital video depth = 0.25(m), wave height = 0.05 (m), frequency = 0.78(sec).



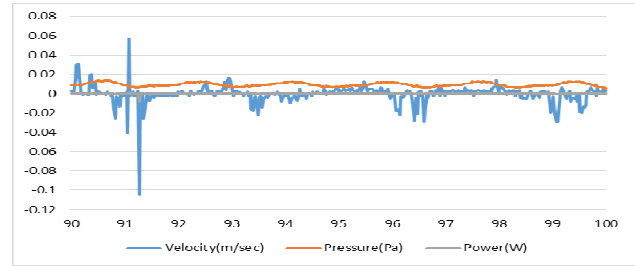
(a) $H = 0.01, T = 0.78, \text{depth} = 0.25$



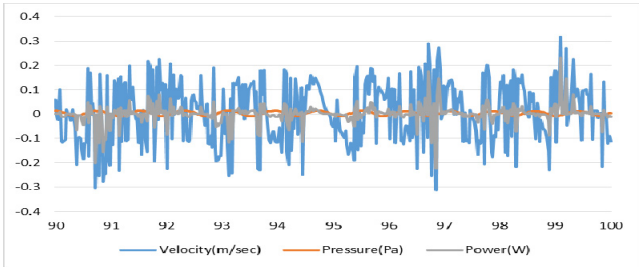
(e) $H=0.05, T = 1.01, \text{depth} = 0.25$



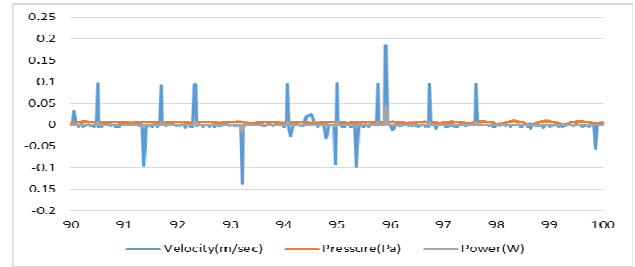
(b) $H = 0.03, T = 0.78, \text{depth} = 0.25$



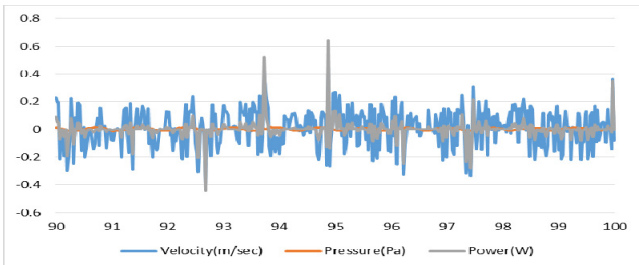
(f) $H = 0.05, T = 1.74, \text{depth} = 0.25$



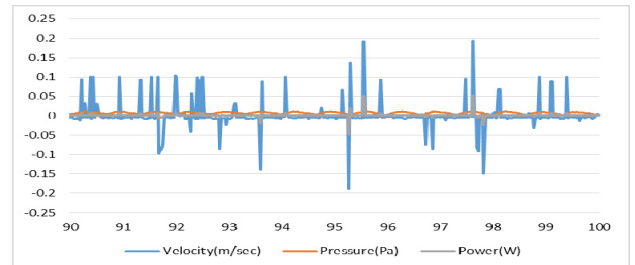
(c) $H = 0.07, T = 0.78, \text{depth} = 0.25$



(g) $H = 0.05, T = 0.58, \text{depth} = 0.25$



(d) $H = 0.09, T = 0.78, \text{depth} = 0.25$



(h) $H = 0.05, T = 0.66, \text{depth} = 0.25$

Figure 5. Power, velocity and pressure time history at the center of the chamber of this model.

As clearly shown in Figure 5, when the frequency increases, the energy remains the same.

Table.1 can be further deduced that the inclined wave height may be adjusted to augment the wave energy, and thus the overall efficiency of an OWC, but wave height = 0.03 m, 0.05 m are small because incident wave be prevented outside of OWC. Table.2 can be further deduced that the inclined wave frequency may be adjusted to augment the wave energy, and thus the overall efficiency of an OWC.

Table 1. Simulated waves considered.

Wave frequency = 0.78(sec), depth = 0.25(m)					
Wave height (m)	0.01	0.03	0.05	0.07	0.09
Average power (W)	0.000092	0.000009	0.000059	0.000281	0.000763

Table 2. Simulated waves considered.

Wave height = 0.05(sec), depth = 0.25(m)					
Wave frequency(sec)	0.58	0.66	0.78	1.01	1.74
Average power(W)	0.000152	0.000332	0.000052	0.000083	0.000021

4. Conclusion

The use of renewable energy is becoming indispensable to support people's way of life, lower emissions of greenhouse gases, and decrease the consumption of natural resources. The water flow in the OWC chamber was determined using pressure and velocity measurements. The water velocities in the chamber during the upward motion of water as a result of wave impact in the column are always larger than those during the downward motion. The data acquired from the video sequences has been used in conjunction with an energy model of the OWC to lend useful insight into its performance. Of course, wave-energy technologies are still to a lesser or greater degree experience. However, the potential for improvement of the wave-energy conversion technologies is large. The survivability and the reliability of many devices, especially for offshore operation, are yet to be demonstrated. Average power is height when wave frequency is small but wave height is height.

Conflict of Interest

Authors state no conflicts of interest.

References

1. Paixao Conde JM, Gato LMC (2008) Numerical study of the air-flow in an oscillating water column wave energy converter. *Renewable Energy* 33: 2637–2644.
2. Folley M, Curran R, Whittaker T (2006) Comparison of LIMPET contra-rotating Wells turbine with theoretical and model test predictions. *Ocean Eng* 33: 1056–69.
3. Marine Renewable Energy (Wave and Tidal) Opportunity Review,[Online]. Available from: <http://www.oceanrenewable.com/wp-content/uploads/2007/03/orereport.pdf>.
4. Bahaj A (2011) Generating electricity from the oceans. *Renew Sustain Energy Rev* 15: 3399–3426.

5. Ocean Energy Systems, Ocean Energy Systems, [Online]. Available from: http://www.ocean-energy-systems.org/ocean_energy/.
6. Ocean Energy, Low Carbon Green Growth Roadmap for Asia and the Pacific, [Online]. Available from: http://www.unescap.org/esd/environment/lcgg/documents/roadmap/case_study_fact_sheets/Fact%20Sheets/FS-Ocean-energy.pdf.
7. Harnessing Energy from the Oceans, Environment News Network, [Online]. Available from: http://aceer.uprm.edu/pdfs/harnessing_energy_oceans.pdf.
8. Chou FNF, Chang CY, Chen YY, et al. (2014) Experiment test of an oscillating water column device of wave energy converter. Conference on Chinese of Mechanical Engineering.



AIMS Press

© 2015 Chia-Ying Chang, et al., licensee AIMS Press. This is an open access article distributed under the terms of the Creative Commons Attribution License (<http://creativecommons.org/licenses/by/4.0>)